A circadian transcriptional sub-network and *EARLY FLOWERING 3* control timing of senescence and grain nutrition in bread wheat

Christopher R. Buckley[1] (0000-0002-4095-2300), Joshua M. Boyte[1] (0009-0005-7495-5058), Robert L. Albiston[1], Jessica Hyles[2] (0000-0002-1836-4334), Jesse T Beasley[1] (0000-0001-7116-3622), Alexander AT Johnson[1] (0000-0002-1209-6447), Ben Trevaskis[2] (0000-0001-7277-4994), Alexandre Fournier-Level[1] (0000-0002-6047-7164), Michael J. Haydon[1] * (0000-0003-2486-9387)

[1]School of BioSciences, University of Melbourne, Parkville, VIC 3010, Australia
[2]CSIRO Agriculture and Food, GPO Box 1700, Canberra, ACT 2601, Australia
* Corresponding author: m.haydon@unimelb.edu.au

Keywords

Triticum aestivum, circadian clock, leaf senescence, GPC, chronotype, grain nutrition

Abstract

Circadian clocks control daily and seasonal timing of physiology and development. Because of their influence on photoperiodic flowering, variants in circadian clock genes have been selected for phenology during domestication of cereal crops. To explore the potential impact of this genetic variation on circadian-regulated traits, we investigated the relationship of the circadian clock and leaf senescence in hexaploid bread wheat. Phenotyping of a collection of elite wheat cultivars identified significant variation in circadian rhythms which was associated with timing of senescence and nutrient mobilisation efficiency. RNA sequencing revealed substantial reorganisation of the circadian-regulated transcriptome during senescence and a transcriptional sub-network representing a link between the circadian oscillator and regulators of leaf senescence. We used genotypes of multiple circadian clock genes to assign cultivars to 'chronotypes', which could be used to predict circadian-regulated phenotypes. This identified a deletion variant of *EARLY FLOWERING 3-D1 (ELF3-D1)* attributed to a phenology locus, *Earliness per se (Eps-D1),* and we used near-isogenic lines (NILs) to show that it affects timing of senescence and grain protein content (GPC). Thus, there are potential consequences of circadian clock genes selected for phenology on other valuable crop traits.

Introduction

Leaf senescence is a controlled process involving the degradation of chlorophyll, downregulation of photosynthesis and the transport of remobilised nutrients to nascent tissues (Gan and Amasino, 1997). Efficient mobilisation of nutrients from vegetative to reproductive tissues during leaf senescence is a key determinant of plant fitness. The relative timing of senescence affects a trade-off between resource accumulation and usage (Distelfeld et al., 2014) and can be adjusted to balance these processes for adaptation to different environments (Estiarte and Peñuelas, 2015; Chen et al., 2020; Bucher and Römermann, 2021). In cereal crops, the timing of senescence has a major impact on yield traits. In bread wheat (*Triticum aestivum*), high grain protein content (GPC) is a valuable trait which can be achieved with earlier senescence, but typically comes at a cost of lower yield (Simmonds, 1995). Furthermore, these relationships can be environment-dependent (Christopher et al., 2016; Christopher et al., 2018; Alhabbar et al., 2018). Increasing nutrient content without yield loss across multiple environments is a priority target for crop breeding.

The circadian clock is a biological timing mechanism, comprised of a highly influential gene regulatory network that functions to synchronise development and physiology with daily and seasonal environmental cycles. Plant circadian clocks strongly affect metabolism, transport and signalling underlying growth and development (Sanchez and Kay, 2016). In numerous cereal crops, the role of the circadian clock in photoperiodic flowering has led to widespread selection of circadian clock gene variants (Bendix et al., 2015), although the impact of these variants on other circadian-controlled traits has not been explored.

Since the circadian clock influences timing of senescence in *Arabidopsis thaliana* (Sakuraba et al., 2014; Zhang et al., 2018; Kim et al., 2018), we sought to explore the role of the circadian clock in wheat in controlling leaf senescence and determining grain nutrient content. We compiled a panel of 25 wheat cultivars and found these traits covaried with phenotypic and genotypic variation in the circadian clock. We compared the circadian transcriptomes of mature and senescent flag leaves and used genotypic information for circadian clock genes to define chronotypes within the wheat panel. These suggested a role for the clock gene *EARLY FLOWERING 3-D1* (*ELF3-D1*) and using near isogenic lines (NILs) of a widespread deletion variant in *ELF3-D1,* we found a functional contribution to timing of senescence and GPC.

Material and Methods

Plant materials

Phenotyping experiments in year one and two used a panel of 15 elite Australian wheat cultivars (Calingiri, Cobra, Corack, Gladius, Hydra, Mace, Magenta, Scout, Sunguard, Suntop, Supreme, Viking, Wyalkatchem, Yitpi and Zen) which were obtained from Australian Grains Genebank (AGG). In the third and fourth years, a 25-cultivar circadian diversity panel was developed by including cultivars from the OzWheat diversity panel developed by the Commonwealth Scientific and Industrial Research Organisation (CSIRO). These additional cultivars were Axe, Bayonet, Buckley, Cascades, EGA Wedgetail, Insignia, Lillimur, Takari, Wilgoyne and Yarralinka.

Four pairs of NILs with variation at *TaELF3-D1* were derived from a large NIL population with phenology gene variation developed by CSIRO (Boden et al., 2015; Steinfort et al., 2017). The NILs were generated by crossing donors of phenology genes with the cultivar Sunstate, which carries the *TaELF3-D1del* allele. This was followed by five rounds of recurrent backcrossing to obtain average 97% genetic identity between NILs.

Growth conditions

For glasshouse experiments, seeds were sown in July-August (Parkville, Victoria). Growth room and growth cabinet experiments were set to 12 h light (200-280 µmol m^{-2} s^{-1}, 20ºC), 12 h dark (15ºC). In all phenotyping experiments, seeds were chilled at 4°C for 48 h and sown in a mix of sterilised potting soil with 4.5 g/L Osmocote 6-9 month slow-release fertiliser. Full details of growth conditions can be found in Supplemental Methods.

Delayed leaf fluorescence (DF) imaging

Unless specified otherwise, DF was imaged in the second leaves of plants at the 5-leaf stage. In all experiments, 2.5 cm sections were dissected from excised leaves (cut 3 cm from the leaf tip) and placed on 12 cm^2 0.5% agar (type M; Sigma-Aldrich) Petri plates, arranged according to a randomised controlled block design. Leaf sections were imaged using a Retiga LUMO charge-coupled device (CCD) camera (Teledyne Photometrics) fitted with a 25 mm f/0.95 lens housed within light-tight dark boxes. Light (>45 µmol $m^{-2}s^{-1}$) was provided by two LB3 red/blue LED panels (Photek). The lights and camera were controlled by beanshell (bsh) scripts in µManager (version 2.0 (Edelstein et al., 2014)). DF was measured in 120 h of continuous light (LL) conditions by 1 min camera exposure in the dark, following 59 min of light. Camera properties were binning =

100 4x4, gain = 1, readout rate = 0.650195 MHz 16 bit. DF was measured in leaf sections from image
101 stacks as integrated density using ImageJ (NIH). Timeseries data were uploaded to BioDare2
102 (Zielinski et al., 2014) for period analysis of background-subtracted data using the fast Fourier
103 transform non-linear least squares (FFT-NLLS) method (Plautz et al., 1997). Data were detrended
104 according to the amplitude and baseline detrending method and analysis was performed using a
105 24 - 96 h window. Estimates of period that fell outside of the range of 24 h ± 5 h or had relative
106 amplitude error (RAE) > 0.6 were excluded. Time series intensity data presented are Z-score
107 normalised.
108
109 *Quantifying time to senescence*
110 Leaf chlorophyll content was recorded using a handheld SPAD meter (Konica Minolta).
111 Measurements were taken three times/week from heading (full emergence of ear). In year two,
112 five SPAD values per plant were measured from the midpoint of the flag leaf of the main tiller and
113 the median value was recorded. In year four, ten SPAD values per plant were measured across
114 the whole flag leaf of the main tiller and the mean value was recorded. Time to senescence was
115 defined as the number of days after anthesis (DAA) to reach 50% of the maximum chlorophyll
116 content. Plants with time to senescence values three standard deviations above or below the
117 overall mean were excluded.
118
119 *Nutrient profiling of grain and leaf samples*
120 Whole flag leaves were harvested at anthesis from six plants of each genotype and mature grains
121 were harvested from another six plants. Flag leaf harvest was performed between 9 am and 12
122 pm (approximately 2-5 h after dawn). For grain samples, all ripened grain heads from each plant
123 were harvested. Thousand grain weight (TGW) was recorded by counting and weighing 50 seeds
124 from each sample. Leaf and grain samples were dried at 65°C for 7 days. Threshed grain samples
125 were sieved with a 2 mm slotted sieve and then milled with a Tube Mill 'Control' (Ika). Each sample
126 was ground for 90 seconds at 25,000 rpm. Dried leaf samples were milled using a TissueLyser
127 (Qiagen), with each sample milled for 2 min at 21.5 Hz with a single 18 mm stainless steel ball
128 bearing. Powdered leaf and grain samples were digested in HNO_3 and ion concentration was
129 determined by inductively coupled plasma optical emission spectroscopy (ICP-OES). Total
130 remobilisation efficiency was calculated as the mean normalised ratio of seed-to-leaf
131 concentration across eight elements (P, S, K, Ca, Mg, Fe, Zn, Mn). Total protein of grain samples
132 was extracted following the protocol of Dupont et al. (2011) and quantified by bicinchoninic acid
133 (BCA) assay.

134

135 *Defining chronotypes*

136 Clock gene markers were identified by searching for SNPs in the OzWheat diversity panel (Hyles,
137 2021). Genotyping of the entire OzWheat panel has been performed with allele-specific markers
138 for agronomically important genes for phenology (e.g. *Ppd-1* and *ELF3*) and around 26K SNPs
139 were identified by transcriptome sequencing (crown tissue from seedlings) of the panel. The
140 OzWheat polymorphism database was filtered against a set of putative wheat clock genes
141 (Supplemental Table 1), and novel non-synonymous SNPs in clock genes were retained.
142 Kompetitive allele specific PCR (KASP) genotyping of clock gene markers (*TaPpd-B1, TaPpd-*
143 *D1, TaELF3-D1*) and novel SNP markers (*TaPRR73-A1, TaPRR59-B1, TaTOC1-B1, TaLUX-B1*)
144 was completed for the circadian diversity panel. Homoeologue-specific primers for each clock
145 gene marker were designed using PolyMarker (Ramirez-Gonzalez et al., 2015) (Supplemental
146 Table 6).

147

148 Genotype data for the seven clock gene markers from cultivars in the OzWheat panel plus
149 additional cultivars in this study were used as input for *k*-modes categorical clustering, using only
150 cultivars with complete genotypic data for the seven genes. To choose the value for *k*, the total
151 within-cluster simple-matching distance was calculated and plotted for a range of possible values
152 of *k* (2–10). *k*-modes clustering was performed using the R/klaR package (Weihs et al., 2005).
153 Chronotypes were visualised in space by multiple correspondence analysis (MCA), performed
154 using the R/FactoMineR package (Lê et al., 2008). To estimate the number of dimensions to
155 retain for MCA, *k*-fold cross-validation was performed using the R/missMDA package (Josse and
156 Husson, 2016), and the number of dimensions (3) that produced the smallest mean square error
157 of prediction (MSEP) was used for MCA.

158

159 *RNA-sequencing*

160 Wheat seeds of the Australian cultivar Mace were sown in a single growth room in two staggered
161 batches, 28 days apart. Leaves were sampled concurrently when 'mature' plants were at ear
162 emergence (Zadok's stage 51-59) and 'senescent' plants had evident chlorophyll degradation in
163 flag leaves. At dawn (*Zeitgeber* Time 0; ZT0), the growth room was set to continuous light and
164 temperature (20ºC) and whole flag leaves from the primary tiller of four plants were collected
165 every 2 h from ZT45 to ZT91 (48 h). Samples were immediately flash frozen in liquid nitrogen and
166 stored at -80°C.

167

168 Frozen leaf tissue was ground to a fine powder in liquid nitrogen-cooled mortar and pestles.
169 Lysate buffer was added to the tissue (350 µL per 100 mg of tissue) and the mixture was vortexed
170 immediately. RNA was extracted using ISOLATE II RNA Plant Kit (Meridian Bioscience). RNA
171 from two individual leaf samples was equally pooled to provide two replicates for sequencing.
172 Library preparation and RNA-sequencing was performed by a commercial provider (Azenta).
173 Library preparations were constructed using NEBNext Ultra RNA Library Prep Kit for Illumina
174 (New England Biolabs; NEB). Libraries with different indices were multiplexed and sequenced on
175 an Illumina HiSeq platform (Illumina, San Diego, CA). Sequencing was carried out using a 2x150-
176 bp paired-end (PE) configuration. An average of 24 million 150-bp PE reads were generated for
177 each library.
178
179 Reads were filtered for quality and mapped to the *T. aestivum* cv. Mace (PGSBv2.1) genome
180 sequence and annotation using STAR with default parameters (Dobin et al., 2013). Mapped reads
181 were quantified and normalised using the cuffquant and cuffnorm modules of Cufflinks (Trapnell
182 et al., 2010). Normalised counts (fragments per kilobase transcript per million reads; FPKM)
183 outputted from cuffnorm were used for downstream analyses. Only transcripts that were
184 expressed (i.e. FPKM > 0) at least once in each 24 h period (ZT45-ZT67 and ZT69-ZT91) were
185 retained.
186
187 *Parameterisation of transcript circadian rhythms*
188 The packages BIO_CYCLE (Agostinelli et al., 2016) and r/MetaCycle (Wu et al., 2016) were used
189 to estimate rhythmicity and parameterise circadian rhythms of transcripts. BIO_CYCLE was run
190 using default parameters, with minimum and maximum expected period values of 20 and 28 h.
191 MetaCycle incorporates different methods for rhythmicity detection to generate a combined
192 prediction of rhythmicity. JTK_CYCLE and Lomb-Scargle (LS) were selected for integration by
193 MetaCycle. Default settings were maintained for all other parameters. Transcripts with $q < 0.05$
194 were retained from both BIO_CYCLE and MetaCycle, and the intersection of rhythmic genes from
195 these datasets was used for downstream analyses. All circadian rhythm parameter estimates
196 (period, phase, amplitude, periodicity) presented are derived from BIO_CYCLE. Phase values are
197 adjusted to period (phase = phase(24/period)). The mature-to-senescent change in each of these
198 parameters at the gene level (Δperiod, Δphase and Δamplitude) are used for several analyses.
199 ΔPeriod and Δphase are calculated as the difference between the mature and senescent value
200 of these parameters for a given gene (e.g. Mature period - senescent period). ΔAmplitude is the

log ratio of mature and senescent amplitude for a given gene (i.e. log(Mature amplitude: senescent amplitude)).

Gene ontology (GO) term and TF family enrichment analysis

GO terms for the *T. aestivum* cv. Mace (PGSBv2.1) annotation were sourced from Ensembl Plants (Cunningham et al., 2022). r/topGO was used to perform GO enrichment analysis of various gene sets using the 'classic' algorithm (Alexa et al., 2006). Fisher's exact test was selected to compare the enrichment of GO terms in each gene set to a gene universe of 87,493 unique wheat genes with GO term annotations. For enrichment analyses of TF families, Chinese Spring wheat genes annotated as TFs were sourced from https://opendata.earlham.ac.uk/wheat/under_license/toronto/Ramirez-Gonzalez_etal_2018-06025-Transcriptome-Landscape/data/data_tables/ (Ramírez-González et al., 2018). Mace orthologues of each gene were assigned through orthology data available from Ensembl Plants (Cunningham et al., 2022). For enrichment analyses, 2 x 2 contingency tables were built for each TF family and analysed with Fisher's exact test (from r/stats). Enrichment analysis of TF families that are only rhythmic in senescent tissue was performed against all rhythmic TFs (rhythmic in senescent, mature or both). Enrichment analysis of differentially rhythmic TFs was performed against all rhythmic TFs (rhythmic in both tissues).

Cis-regulatory element enrichment

Promoter sequences (1000 bp upstream of the start codon) were obtained from all wheat genes using the 'retrieve sequences' tool from RSAT (Regulatory Sequence Analysis Tools) (Nguyen et al., 2018). Promoter sequences were subsetted into groups of interest (e.g. short period genes), and these groups were used as input for *cis*-regulatory element enrichment analysis. For this, promoter sequences from the target set of genes were used as input for RSAT peak-motifs oligo-analysis (Thomas-Chollier et al., 2012), with all genes that were rhythmic in either mature or senescent flag leaves used as the control set. Peak-motifs settings were kept as default, and significantly enriched oligos with E-value < 0.05 were retained. For each significantly enriched oligo, motif matching was performed with STAMP (Similarity, Tree-building, and Alignment of Motif Profiles) (Mahony and Benos, 2007) against the PLACE database of plant motifs (Higo et al., 1998), using default settings. The top match for each oligo (with smallest *p*-value) was retained.

Differential expression and differential rhythmicity

235 LimoRhyde (linear models for rhythmicity, design) was used to test for statistically significant
236 changes in rhythmicity between mature and senescent tissue (differential rhythmicity; DR) (Singer
237 and Hughey, 2019). LimoRhyde first decomposes *Zeitgeber* Time into sine and cosine with a
238 period of 24 h. Then, transcripts that exhibit DR are identified using a linear model that tests for
239 significant interactions between developmental stage and the time components. LimoRhyde was
240 also used to identify differentially expressed (DE) transcripts. For this, a linear model tests for
241 interactions between developmental stage without interaction of the time components(Singer and
242 Hughey, 2019). Code used to perform LimoRhyde's functions was developed from a vignette from
243 the LimoRhyde GitHub repository (https://github.com/hugheylab/limorhyde). *p*-values were
244 adjusted by the Benjamini-Hochberg procedure with a false discovery rate FDR = 5% (Benjamini
245 and Hochberg, 1995). DR and DE genes were assigned using a *q*-value threshold of 0.05. DE
246 genes have log2(fold change) > 1.2 or < -1.2. To allow comparison of circadian rhythm parameters
247 (i.e. period, phase, amplitude), the DR gene set was filtered against the set of genes that are
248 rhythmic in both tissues.
249
250 *STRING protein-protein network analysis*
251 Protein-protein interactions of DR wheat TFs were analysed using STRING (Szklarczyk et al.,
252 2023). STRING uses an early genome assembly and annotation for wheat (CSS; International
253 Wheat Genome Sequencing Consortium (IWGSC), 2014). CSS gene IDs for the DR gene list
254 were acquired via BLAST searches within STRING, though not all Mace gene annotations had
255 an equivalent locus in the CSS assembly. DR TFs with STRING entries were used to build a
256 protein-protein network in STRING. The network was built using both physical and functional
257 protein interactions, and the minimum weighted interaction score was set to 0.4.
258
259 *Clustering of oscillator transcript responses*
260 Mace orthologues of putative wheat circadian oscillator genes from Chinese Spring were
261 identified using orthology data from Ensembl Plants (Cunningham et al., 2022) (Supplemental
262 Table 2). The list of genes was filtered to include only transcripts that are rhythmic in both mature
263 and senescent tissue. Principal component analysis (PCA) was performed for the 59 clock genes
264 in this list using three variables: mature-to-senescent changes in circadian period, phase, and
265 amplitude (Δperiod, Δphase and Δamplitude). The three PCs from this analysis were used as
266 input for *k*-means clustering. To determine an optimal value of *k*, the ratio of within-cluster sum-
267 of-squares (WCSS) to total sum-of-squares (TSS) was plotted against a range of potential *k*
268 values (1-8). PCA and *k*-means were performed using r/stats.

Results

Circadian period and timing of senescence covary in Australian wheat cultivars

Since the circadian clock influences leaf senescence in Arabidopsis (Sakuraba et al., 2014; Zhang et al., 2018; Kim et al., 2018) and the pace of circadian rhythms shortens with age (Kim et al., 2016; Rees et al., 2019), we investigated the relationship between phenotypic variation of circadian rhythms in wheat and the timing of senescence. Using delayed leaf fluorescence (DF) (Figure 1A), we first measured circadian rhythms in the second leaf of three wheat cultivars 14 days after sowing (DAS; seedling), 33 DAS (5-leaf stage) and 44 DAS (end of tillering). Relative amplitude error (RAE; a proxy for rhythm robustness) did not significantly differ by leaf age (Figure 1B), but circadian period was significantly shorter in leaves of older plants (Figure 1C). This demonstrates that changes occur in the circadian clock of wheat plants during ageing.

To assess the extent of phenotypic variation of circadian rhythms in wheat, we chose 15 elite cultivars grown across diverse environments of Australia (Supplemental Figure 1) and measured circadian rhythms of DF in glasshouse-grown plants in two years. Significant differences in mean circadian period were detected between cultivars in each year (Figure 1D, Supplemental Figure 2A, Supplemental Data 1). In year 1, mean circadian period differed by over four hours over the panel (Figure 1D,E). Circadian period was mostly consistent within cultivars over both years, except for Viking and Scout, which might suggest strong gene-by-environment interactions in these cultivars (Supplemental Figure 2B). Nevertheless, there is robust variation in circadian rhythms within elite wheat germplasm which could influence circadian-regulated agronomic traits.

To measure the timing of senescence in the 15 wheat cultivars, we monitored the decline of chlorophyll content in flag leaves after anthesis (Supplemental Data 1). There were significant differences in the timing of senescence between cultivars (Figure 1F), with a maximum mean difference of 10.3 days. We also measured total ion content of mature flag leaves and harvested grain to calculate nutrient mobilisation efficiency (Supplemental Data 1). We detected substantial variation in mobilisation efficiency between cultivars (Figure 1G; Supplemental Figure 3) and observed a strongly negative correlation with timing of senescence (Supplemental Figure 4). Timing of senescence and nutrient mobilisation efficiency were both significantly correlated with circadian period in year one (Figure 1H,I), such that cultivars with shorter period tended to senesce earlier and had more efficient nutrient mobilisation. The relationship of these traits to circadian period was weaker in year two due to a strong year-effect for Scout and

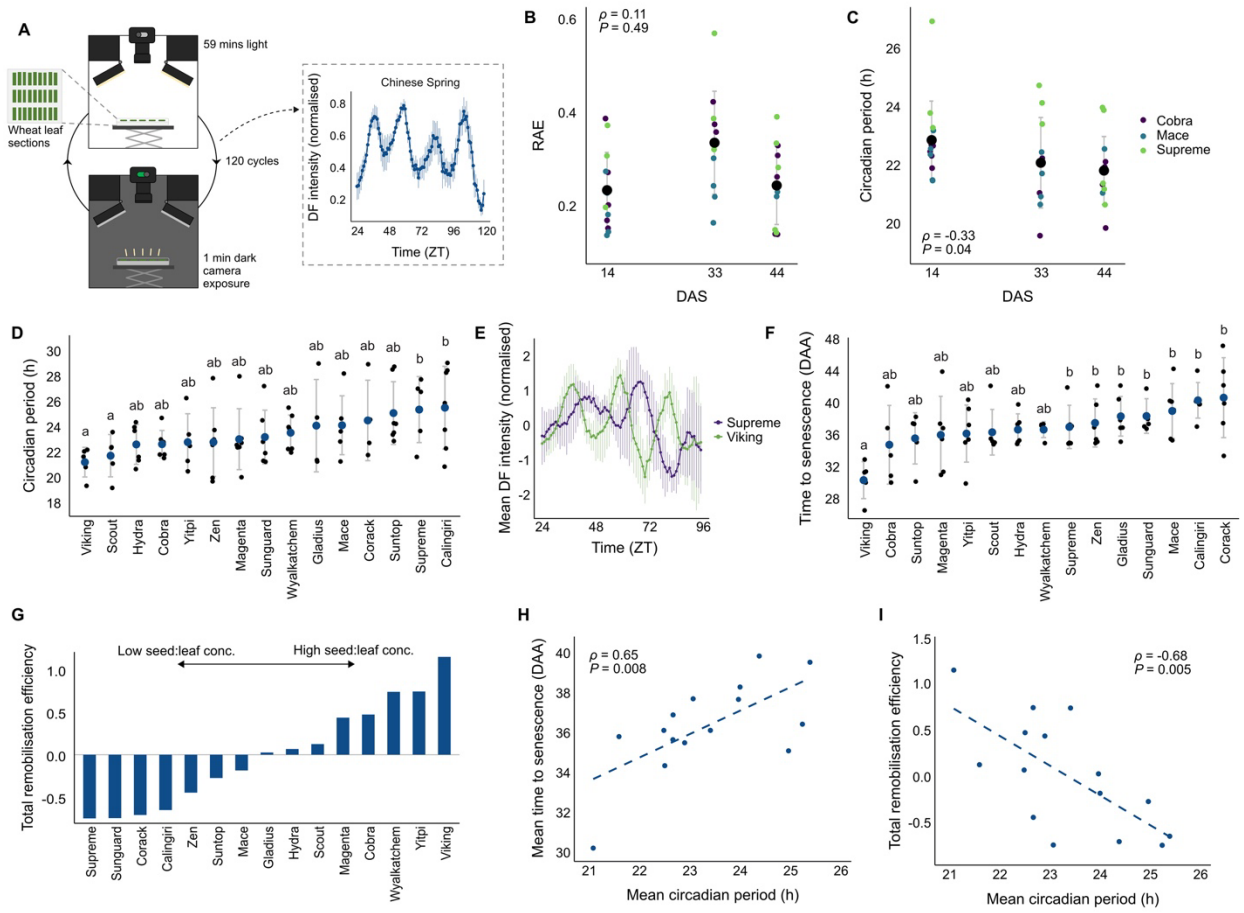

Figure 1: Circadian period of wheat cultivars is associated with senescence and grain nutrition. A, Overview of delayed fluorescence (DF) workflow for measuring wheat circadian rhythms. **B,** Relative amplitude error (RAE) and **C**, circadian period of DF rhythms in 2nd leaf of three cultivars at 14, 33 and 44 days after sowing (DAS). Significance of relationship with age (DAS) assessed by Pearson's product-moment correlation. Error bars represent ±sd, n=15. **D,** Circadian period of DF in 15 Australian wheat cultivars in year one. Letters indicate significant differences as determined by Welch's *t*-test, $P < 0.05$. Error bars represent ±sd, n=8. **E,** Circadian rhythms of DF in the Supreme and Viking. Error bars represent ±sd, n=8. **F,** Time to senescence, (days after anthesis; DAA) in 15 wheat cultivars. Letters indicate significant differences as determined by one-way ANOVA followed by Tukey's HSD; $P < 0.05$. Error bars represent ±sd, n=6. **G,** Total nutrient remobilisation efficiency (ratio of leaf-to-seed nutrient content, see methods) in 15 wheat cultivars. **H**, Mean circadian period (year one) versus mean time to senescence and **I,** total remobilisation efficiency in 15 wheat cultivars. Significance assessed by Pearson's product-moment correlation.

Viking. Without these cultivars, a stronger correlation was detected (Supplemental Figure 2C,D). We also measured total GPC, an important trait which depends on nutrient mobilisation (Supplemental Figure 5A, Supplemental Data 1). GPC was significantly negatively correlated with

321 circadian period in year two, but not year one (Supplemental Figure 5B,C). Overall, our data
322 suggest strong relationships between circadian period, leaf ageing and senescence, nutrient
323 mobilisation efficiency and GPC in elite wheat cultivars.
324
325 **Reshaping of the circadian transcriptome during leaf senescence**
326 To explore transcriptional changes in the circadian network during leaf senescence we compared
327 the transcriptomes of mature and senescent flag leaves in *cv.* Mace over 48 h in continuous light
328 (Figure 2A). Principal component analysis (PCA) separated each individual transcriptome by
329 developmental stage (Supplemental Figure 6A) and time of day (Supplemental Figure 6B-E). We
330
331 used BIO_CYCLE (Agostinelli et al., 2016) and MetaCycle (Wu et al., 2016) to detect rhythmic
332 transcripts and estimated their period, phase and amplitude (Supplemental Data 2). A total of
333 11,705 expressed transcripts were called rhythmic in mature flag leaves (15.7% of 74550
334 expressed) by both algorithms and 16,906 transcripts were rhythmic in senescent flag leaves
335 (22.8% of 74272 expressed) (Figure 2B). Since fewer rhythmic genes were detected in mature
336 flag leaves compared to senescent flag leaves, the changes in the circadian transcriptome during
337 senescence are unlikely to be due to a general decay in gene expression. We performed gene
338 ontology (GO) enrichment analysis of transcripts that are rhythmic only in senescent flag leaves
339 (Supplemental Data 3). Significantly enriched terms included “protein transport”, “peptide
340 metabolic process” and “nitrogen compound transport” (Figure 2C), suggesting that the circadian
341 network is connected to the reprogramming of metabolism and transport during senescence.
342
343 To identify potential regulators of the circadian transcriptome during leaf senescence, we
344 compared periodicity (BIO_CYCLE’s measure of rhythmicity, from 0 to 1) across families of
345 transcription factors (TFs) (Ramírez-González et al., 2018). *PSEUDO RESPONSE*
346 *REGULATORs* (*PRRs*), which are core circadian oscillator genes (Nakamichi et al., 2005), were
347 the most rhythmic family in both tissue types, followed by Sigma70-like TFs, which regulate
348 rhythmic chloroplast gene expression in Arabidopsis (Figure 2D) (Noordally et al., 2013). Mean
349 periodicity of the *WRKY* and *CCAAT-HAP2* families was significantly higher in senescent tissue
350 than mature tissue (Figure 2D). To summarise the overall changes in TF gene expression, we
351 calculated metagene expression values of entire TF gene families (Figure 2E) and observed a
352 clear increase of *WRKY* metagene rhythmicity during senescence. By contrast, a similar change
353 in rhythmicity was not observed for other TF families with roles in senescence (e.g. *NAC, AP2*
354 and *MYB* (Cao et al., 2023)), although we did detect a phase advance of metagenes for the *MYB,*

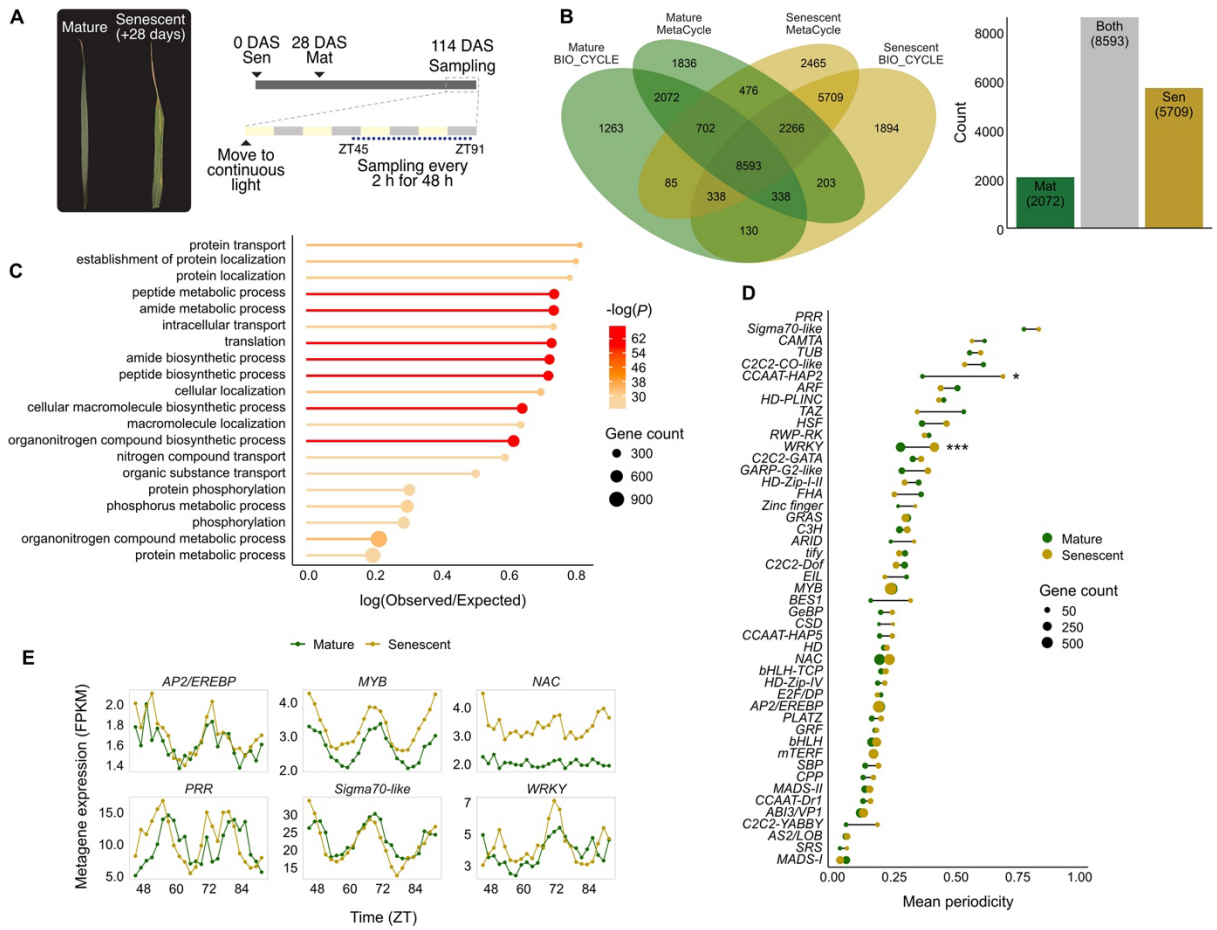

Figure 2: Circadian transcriptional network increases its output at leaf senescence. A, Sampling design of comparative circadian senescence transcriptome. 'Sen' and 'Mat' refer to the sowing dates of plants that were harvested for senescent and mature flag leaves, respectively. **B,** Number of transcripts determined to be rhythmic by BIO_CYCLE (Agostinelli et al., 2016) and MetaCycle (Wu et al., 2016). **C,** Gene ontology term enrichment analysis of transcripts that are uniquely rhythmic in senescent flag leaves. **D,** Comparison of mean periodicity of transcription factor families determined by BIO_CYCLE (0 = arrhythmic). Asterisks indicate significant differences as determined by Welch's *t*-test, * = $P < 0.05$, *** = $P < 0.001$. **E,** Metagene expression (average across entire gene family) of selected transcription factor families.

PRR and *Sigma70* families (Figure 2E). *WRKY* genes are known as regulators of leaf senescence (Guo and Gan, 2005) but our data suggests the influence of the circadian clock on their regulation might have been underestimated.

Among the 8,593 rhythmic transcripts in both tissues, the mean circadian period was ~0.5 h shorter in senescent flag leaves compared to mature flag leaves (Figure 3A; Supplemental Figure 7B). This is consistent with the expectation for shorter period in older leaves (Figure 1C). In

373 addition, a circadian phase advance of ~0.5 h (corrected for period) was also detected in
374 senescent leaves (Supplemental Figure 7A,B). Amplitude differences were small between the two
375 developmental stages, although mean amplitude was higher in mature tissue (Supplemental
376 Figure 7C).
377
378 We noted that there was substantial variation in the period differences for individual transcripts
379 outside the global trend (Figure 3A). To identify patterns in differential period, we performed GO
380 term enrichment of transcripts with shorter (< -0.5 h), longer (> 0.5 h) or unchanged (< ±0.5 h)
381 circadian period in senescent leaves (Supplemental Data 3). Rhythmic genes with shorter period
382 were significantly enriched for GO categories related to primary metabolism (Figure 3B,C;
383 Supplemental Figure 8). Among transcripts with longer period in senescent tissue, terms related
384 to photosynthesis were overrepresented, perhaps reflecting the breakdown of normal rhythmic
385 regulation of photosynthesis (Figure 3B,C; Supplemental Figure 8). The two most strongly
386 enriched GO terms within transcripts with unchanged period were “rhythmic process” and
387 “circadian rhythm” (Figure 3B,C; Supplemental Figure 8). This suggests that the global shortening
388 of period in the senescent transcriptome could be driven by amplitude or phase changes in the
389 circadian oscillator.
390
391 To identify other transcriptional changes between mature and senescent leaves, we used
392 LimoRhyde (Singer and Hughey, 2019) to identify differentially expressed (DE) and differentially
393 rhythmic (DR) genes (Supplemental Figure 9, Supplemental Data 3). Among DE genes in
394 senescent leaves, 6,310 upregulated genes were enriched for GO terms for transport and
395 catabolism, and 8,785 downregulated genes were enriched for GO terms related to biosynthesis
396 (Supplemental Figure 10). There were 1,743 DR genes, enriched for GO terms related to
397 photosynthesis, light signalling and circadian rhythms (Figure 3D). When we compared DR genes
398 to the remainder of the rhythmic transcriptome, we observed an advanced mean phase in
399 senescent tissue, rather than change in period or amplitude (Figure 3E).
400
401 **A circadian-regulated sub-network in senescent leaves**
402 We hypothesised that the phase-advanced DR genes, which are enriched for the “circadian
403 rhythm” GO term, represent a sub-network driving shorter period of the wider transcriptome. We
404 identified 106 TFs among the DR genes (Supplemental Data 3), which were characterised by
405 large phase advances (Supplemental Figure 11A). Several families of TFs were significantly over-
406 represented, including C2C2-Dof, TAZ, FHA, PRR and Sigma70 (Supplemental Figure 11B). To

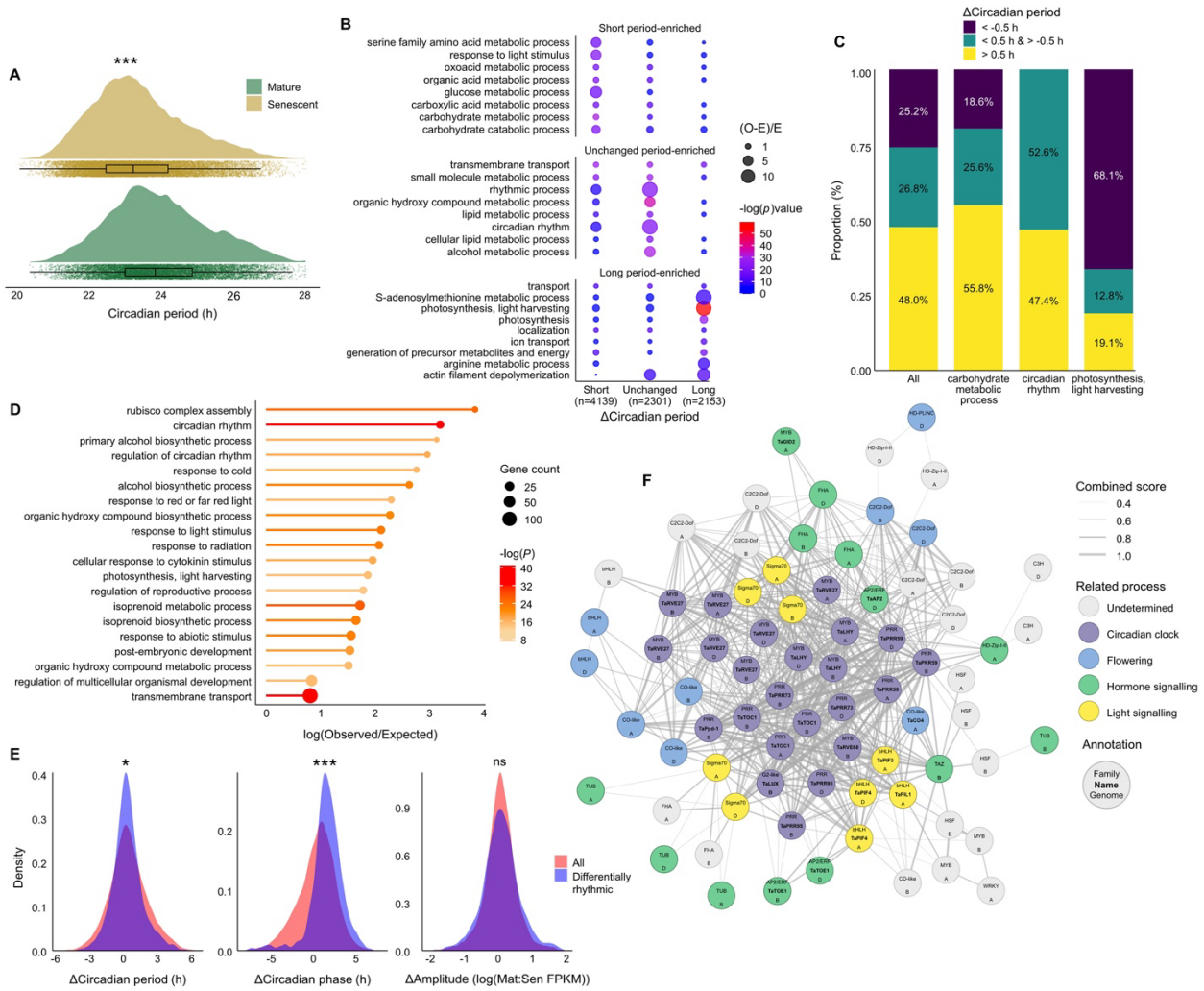

Figure 3: A circadian-regulated transcriptional subnetwork in senescent leaves. A, Distribution of circadian period values of all rhythmic transcripts in mature and senescent flag leaves. Asterisks indicate a significant difference between the mean circadian period values, Welch's *t*-test, $P < 0.001$. **B,** GO term enrichment analysis of transcripts categorised according to the change in circadian period between developmental stages; short period (Δperiod < -0.5 h), long period (Δperiod > 0.5 h), unchanged period (Δperiod < ±0.5 h). O (observed) and E (expected) number of transcripts. **C,** Proportions of transcripts in each Δperiod category for a selection of GO terms. **D,** GO term enrichment analysis of differentially rhythmic (DR) genes. **E,** Distribution of changes in circadian rhythm parameters for DR genes. Asterisks indicate significant differences between DR genes and all other rhythmic genes as determined by Welch's *t*-test, * = $P < 0.05$, *** = $P < 0.001$, ns = not significant. **F,** Putative protein-protein interaction network of DR transcription factors. Combined score reflects the probability of interaction determined by STRING (Szklarczyk et al., 2023). Related processes are manually assigned after literature and orthology database searches.

analyse the interactions between DR TFs, we modelled the putative interactions between members of this gene set using STRING (Szklarczyk et al., 2023). We identified 308 putative

425 functional and physical interactions, which is 7x more than expected (Hypergeo. test, $P < 1x10^{-}$
426 ^{16}). The network includes genes related to hormone signalling, light signalling and photoperiodic
427 flowering, and is centred around core clock genes; *PRRs*, *REVEILLEs* (*RVEs*), *LUX*
428 *ARRHYTHMO* (*LUX*) and *LATE ELONGATED HYPOCTYL* (*LHY*) (Figure 3F). Evening elements
429 (EEs), which are *cis*-regulatory motifs recognised by clock TFs (Harmer et al., 2000), were highly
430 significantly enriched among all DR gene promoters (Supplemental Table 1). These results
431 suggest that there is a circadian-controlled transcriptional subnetwork with advanced phase in
432 senescent tissue.
433
434 We performed a systematic analysis of circadian oscillator gene expression and identified 59 out
435 of 79 putative circadian oscillator genes (Supplemental Table 2) that were rhythmic in both tissues
436 (Supplemental Figure 12). Mean period difference of this group was 0.52 h, which was similar to
437 the global trend, and suggested that maintenance of period is not uniform across the oscillator
438 (Figure 3B). Strikingly, the mean phase advance of oscillator genes was 1.37 h, which is
439 significantly larger than the global average (Welch's *t*-test, t (59.5) = 4.21, $P < 0.001$). To
440 categorise the oscillator genes by rhythmic expression patterns, we performed PCA of changes
441 in period, phase and amplitude (Figure 4A). The three PCs were grouped into six transcript
442 clusters of 1-20 genes by *k*-means (Figure 4C). Clusters 5 and 6 are mainly comprised of genes
443 expressed around dawn, including *RVEs*, *NIGHT LIGHT–INDUCIBLE AND CLOCK-*
444 *REGULATED* (*LNKs*) and *LHY* genes (Figure 4C) and have shorter period in senescing tissue,
445 consistent with the global trend (Figure 4B,D). Clusters 2, 3 and 4 have advanced phase in
446 senescing tissue (Figure 4B), similar to the identified subnetwork (Figure 3F). These are mostly
447 afternoon- or evening-phased genes and include the majority of *PRR* and *LUX* genes (Figure 4C).
448 Amplitude was increased in cluster 2 genes, and period was unchanged in clusters 2 and 4 (Figure
449 4B,D). Thus, there appear to be distinct changes in oscillator genes during senescence according
450 to their phase of expression and this suggests a restructuring of the circadian oscillator during
451 leaf senescence.
452
453 **Identification of chronotypes within elite wheat cultivars**
454 Since the circadian clock appears to strongly influence the wheat transcriptome during leaf
455 senescence, we sought to maximise circadian gene variation within the wheat panel for further
456 phenotyping. We explored SNP data for the OzWheat diversity panel comprised of 283 Australian
457 cultivars. We found four novel non-synonymous SNPs in conserved regions of clock genes from

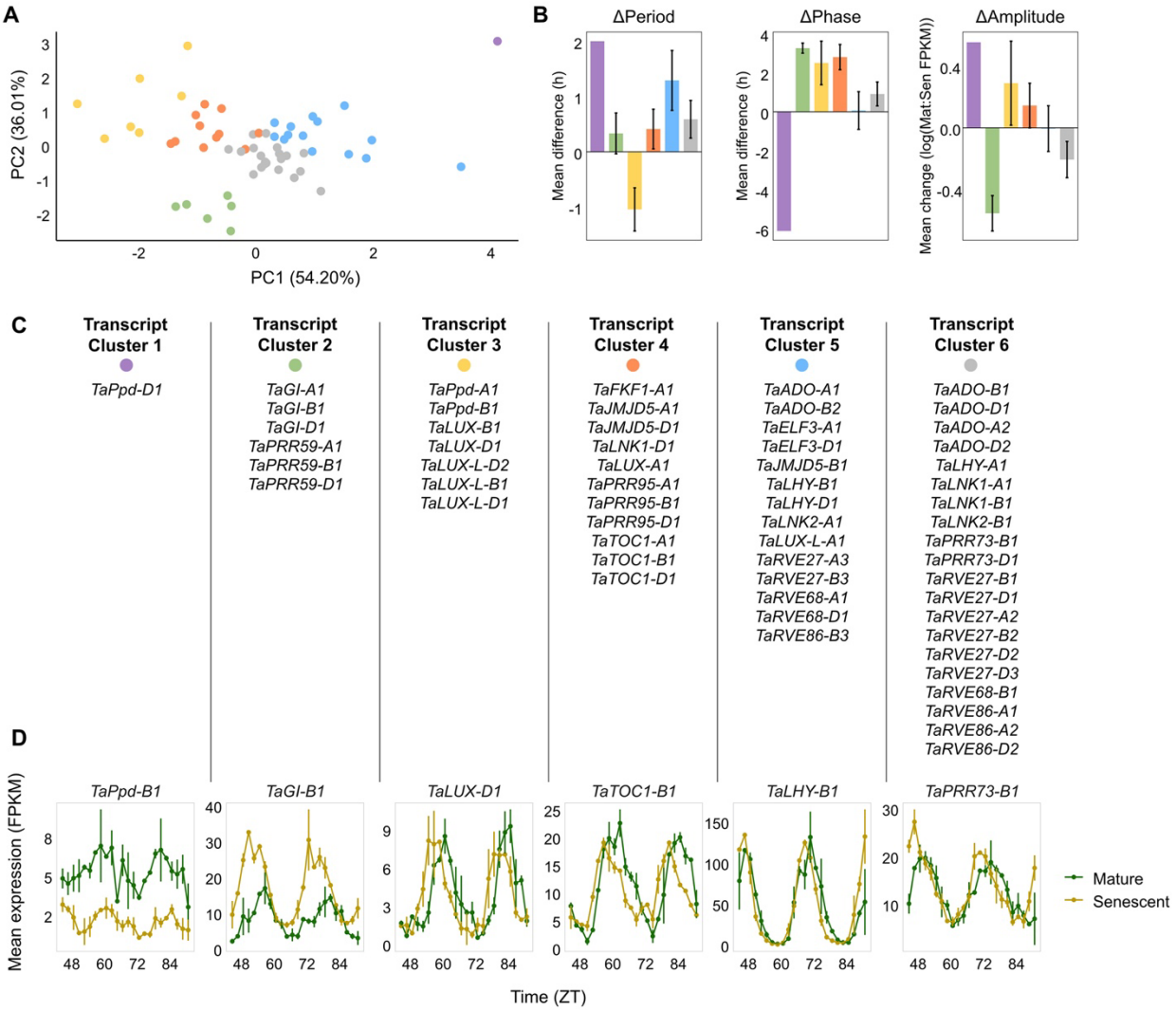

Figure 4: Reshaping of the circadian oscillator during leaf senescence. A, PCA of changes in circadian period, phase and amplitude between mature and senescent leaves for putative circadian oscillator genes. PCs generated were used to group transcripts into 6 clusters (represented by different colours). **B,** Mean change in circadian period, phase and amplitude for each transcript cluster. **C,** Names of genes within each transcript cluster. **D,** Transcript circadian rhythms for a representative gene from each cluster. Error bars represent ±sd.

distinct transcript clusters (Figure 3C); *TaPRR59-B1* (Cluster 2), *TaLUX-B1* (Cluster 3), *TaTOC1-B1* (Cluster 4) and *TaPRR73-A1* (Cluster 6). We used these SNPs and three major polymorphic clock gene loci in wheat (*TaPpd-B1*, *TaPpd-D1* and *TaELF3-D1* (Beales et al., 2007; Cane et al., 2013; Wittern et al., 2023)), to categorise cultivars into six chronotypes (Figure 5A,B; Supplemental Table 3) and compiled a circadian diversity panel of 25 cultivars, representing all six chronotypes (Supplemental Table 4), which were phenotyped for circadian period and timing of senescence (Figure 5E,F; Supplemental Figure 13, Supplemental Data 1). There were

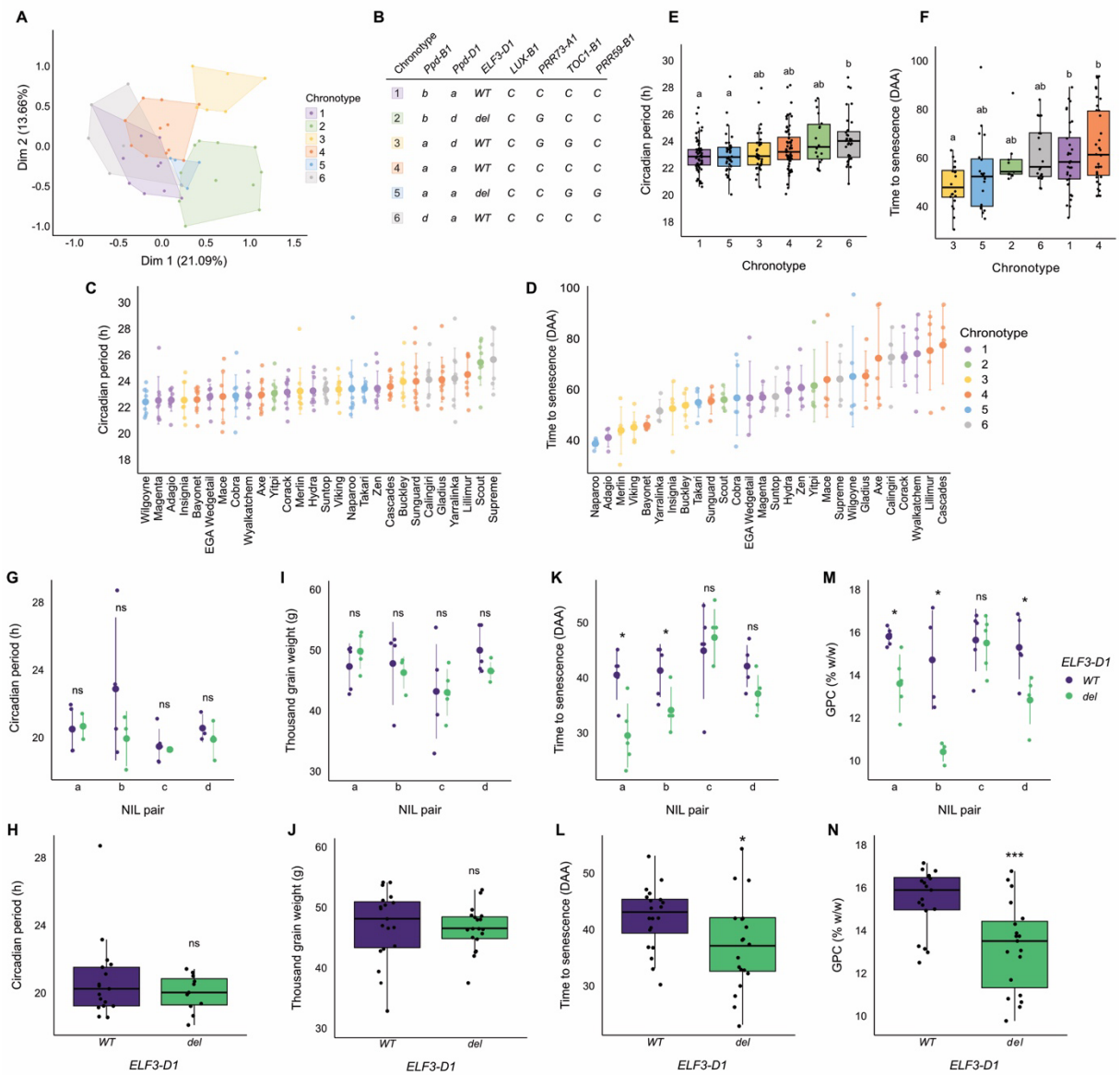

Figure 5: Wheat clock gene variation affects time to senescence and GPC. A, Cultivars from the OzWheat diversity panel were grouped into chronotypes by *k*-modes clustering based on their genotype at seven clock gene markers**.** Multiple correspondence analysis was used to visualise clusters in space. **B,** Mode allelic variation of each cluster (see Supplemental Table 3 for explanation of alleles). **C,** Circadian period (n=10) and **D**, time to senescence (n=5) of 25 wheat cultivars in a circadian diversity panel. Error bars represent ±sd. **E,** Circadian period and **F,** time to senescence for the 25 cultivars by chronotype defined in **A**. Letters indicate significant differences as determined by one-way ANOVA followed by Tukey's HSD; $P < 0.05$. **G,H,** Circadian period, **I,J,** thousand grain weight (TGW), **K,L,** time to senescence and **M,N,** grain protein content (GPC) of near isogenic lines (NILs) for variation at *TaELF3-D1*. Individual NIL pairs are shown in **G,I,K,M.** Error bars represent ±sd, n=5 . Values for all four NILs with functional (*WT*) and *ELF3-D1del (del)* are combined in **H,J,L,N.** Asterisks indicate significant differences between *WT* and *del* alleles as determined by Welch's *t*-test, * = $P < 0.05$, *** = $P < 0.001$, ns = not significant.

487 significant differences between chronotypes for both circadian period and time to senescence
488 (Figure 5C,D). In turn, grain filling was also affected, as thousand grain weight (TGW) differed
489 significantly between chronotypes (Supplemental Figure 14A,B, Supplemental Data 1). However,
490 there were no significant differences between chronotypes for GPC (Supplemental Figure 14C,D,
491 Supplemental Data 1). Although the circadian period values do not correlate with time to
492 senescence and TGW for all chronotypes, chronotype 5 exhibited short period, early senescence
493 and low TGW, while chronotype 6 showed both longer period and later senescence (Figure 5C,D;
494 Supplemental Figure 14).
495
496 ***ELF3-D1* deletion impacts timing of senescence and GPC**
497 Chronotypes 2 and 5 both have a deletion in *TaELF3-D1* and relatively early senescence. To test
498 the potential for this circadian polymorphism on timing of leaf senescence, we used four pairs of
499 near-isogenic lines (NILs) that differ by variation at *TaELF3-D1* (Supplemental Table 3,4,
500 Supplemental Data 1). Across the four pairs of NILs circadian period was not significantly different
501 (Figure 5G,H) and neither was TGW (Figure 5I,J). However, early senescence was detected for
502 the *TaELF3-D1* deletion in three out of four NIL pairs (Figure 5K,L). Similarly, GPC was reduced
503 by the *TaELF3-D1* deletion in the same three NIL pairs (Figure 5M,N). The exception is NIL pair
504 c, which carries a different genotype for *TaPpd-D1* (Supplemental Table 5), a putative
505 downstream target of *ELF3*. Thus, the absence of an effect in this NIL pair could be explained by
506 an epistatic interaction.
507
508 **Discussion**
509
510 We have used a diverse collection of elite wheat cultivars and comparative transcriptomics to
511 explore the relationship between circadian clock function and the process of leaf senescence in
512 wheat and assess its impact on grain quality. Our data reveal significant phenotypic variation in
513 circadian rhythms within wheat cultivars and identify strong correlations with timing of leaf
514 senescence, nutrient mobilisation efficiency and GPC. Comparison of the circadian transcriptome
515 in mature and senescent leaves identified a circadian-controlled subnetwork, centred around
516 several core clock genes and connected to possible transcriptional regulators of senescence.
517 Using genotypic information for circadian clock genes in these wheat cultivars we were able to
518 define chronotypes which we show could potentially be used to predict circadian phenotypes and
519 yield traits. Phenotyping of NILs for an extant deletion variant in *TaELF3-D1* revealed a functional
520 contribution of this core circadian clock gene to timing of senescence and GPC.

521

522 ELF3 is a core component of the circadian oscillator as part of the evening complex (EC), a
523 transcriptional repressor complex also comprised of ELF4 and LUX in Arabidopsis (Nusinow et
524 al., 2011). Null mutants in *ELF3* in Arabidopsis and double null mutants in tetraploid wheat have
525 arrhythmic circadian phenotypes (Hicks et al., 1996; Wittern et al., 2023). Hypomorphic alleles of
526 *elf3* in Arabidopsis have short period phenotypes (Kolmos et al., 2011; Anwer et al., 2014).
527 Chronotypes 2 and 5 have a *TaELF3-D1* deletion, and chronotype 5 had a relatively short period
528 (Figure 5). Since we did not detect significant differences between the *TaELF3-D1* NIL pairs, it
529 seems unlikely that this variant alone causes the short period phenotype. Notwithstanding that
530 the *TaELF3-D1* deletion might be recessive to functional A and B homoeologues for circadian
531 period, there are several genotypic differences in clock genes between these two chronotypes,
532 so the short period of chronotype 5 could be due to genetic interactions between different clock
533 alleles. For example, chronotypes 2 and 5 have different alleles at *TaPpd-D1* and *TaPpd-B1*,
534 which are putative regulatory targets of the EC (Alvarez et al., 2023).
535
536 We found a significant effect of the *TaELF3-D1* deletion on timing of leaf senescence and GPC
537 for three out of four NIL pairs (Figure 5). This suggests that the widespread *TaELF3-D1* deletion,
538 attributed to *Earliness per se (Eps-D1)* locus (Zikhali et al., 2016; Wittern et al., 2023), has a
539 potential negative effect on grain quality, independent of any effect on circadian period. The
540 exception was NIL pair c, which has a promoter deletion within *TaPpd-D1,* in contrast to the
541 functional alleles present in the other three (Supplemental Table 5). Thus, the effect of *TaELF3-*
542 *D1* on senescence might depend on the genotype at *TaPpd-1.* Notably, *TaPpd-B1* is among the
543 *PRR* genes identified within the transcriptional subnetwork (Figure 3) which we predict to make a
544 regulatory contribution to leaf senescence.
545
546 Increased GPC is commonly associated with reduced yield in cereal crops (Simmonds, 1995) and
547 this relationship has been attributed to timing of senescence (Distelfeld et al., 2014). TGW, which
548 is an important yield component, was not significantly different between *TaELF3-D1* NILs (Figure
549 5), but accurate estimates will require multi-year field trials. These will also be required to better
550 assess the robustness of the relationship between circadian period and timing of senescence,
551 since we detected substantial gene-by-environment effects for some cultivars (Supplemental
552 Figure 2).
553

554 The overall trend in the rhythmic transcriptome was of shorter circadian period in senescent tissue
555 (Figure 3) which is consistent with expectations of accelerating rhythms with age (Kim et al., 2016;
556 Rees et al., 2019) (Figure 1). However, there was substantial variation across the transcriptome.
557 For example, photosynthesis genes had a longer period, which could be explained by general
558 decay in expression and an uncoupling from the core oscillator. Of particular note, genes that
559 were relatively unchanged for period were enriched for circadian genes and instead are
560 characterised by an advanced phase (Figure 3). Indeed, three of the circadian transcript clusters
561 we defined had advanced phase in senescent tissue, and include numerous *PRR* genes, EC
562 genes and *GIGANTEA* (Figure 4). We propose that the phase adjustment of these oscillator
563 genes could be driving the period change of the wider transcriptome. Interestingly, *ELF3* genes
564 and *TaPpd-D1* are among the few oscillator genes that have a substantially shorter period in
565 senescent leaves and might represent a regulatory link between the adjusted oscillator and
566 senescence-regulated genes.
567
568 Our findings have potentially important implications for breeders and growers because they
569 suggest that extant variation in circadian clock genes in crops, which were selected for their
570 effects on phenology, can have a significant impact on other traits such as grain quality. The
571 extent of these effects is likely to depend on genetic interactions between other circadian loci and
572 so identifying chronotypes within wheat germplasm could be a useful tool to predict phenotypic
573 effects. The TFs within the subnetwork are candidates that could be targeted to fine-tune
574 circadian-regulated leaf senescence without affecting the core circadian clock.
575
576 **Acknowledgements**
577 We thank Tina Rathjen for her help with genotyping and genetic analysis and Vanessa Melino for
578 sharing seed. Research was funded by the Research Continuity Scheme from the Faculty of
579 Science, University of Melbourne and the JN Peters Bequest to MJH, and an Alfred Nicholas
580 Fellowship, Melbourne Research Scholarship and Faculty of Science Postgraduate Writing-Up
581 Award to CRB. This research was not funded by the Australian Research Council. Generation of
582 NILs at CSIRO was supported by GRDC project CSP00183.
583
584 **Competing interests**
585 The authors declare no competing interests.
586
587

588 **Author contributions**

589 MJH conceived the study, CRB and MJH designed experiments, CRB, JMB, RLA and MJH
590 performed experiments, CRB, JH, AFL and MJH analysed data, JH, JTB, AATJ, BT and AFL
591 provided expertise and resources, CRB and MJH wrote the manuscript, JH, BT and AFL reviewed
592 and edited the manuscript.

593

594 **Data availability**

595 Sequencing data have been deposited in NCBI Gene Expression Omnibus (GSE259431).

596

597 **References**

598

599 **Agostinelli, F., Ceglia, N., Shahbaba, B., Sassone-Corsi, P., and Baldi, P.** (2016). What time
600 is it? Deep learning approaches for circadian rhythms. *Bioinformatics* **32**:i8–i17.

601 **Alexa, A., Rahnenführer, J., and Lengauer, T.** (2006). Improved scoring of functional groups
602 from gene expression data by decorrelating GO graph structure. *Bioinformatics*
603 **22**:1600–1607.

604 **Alhabbar, Z., Islam, S., Yang, R., Diepeveen, D., Anwar, M., Balotf, S., Sultana, N.,**
605 **Maddern, R., She, M., Zhang, J., et al.** (2018). Associations of NAM-A1 alleles with the
606 onset of senescence and nitrogen use efficiency under Western Australian conditions.
607 *Euphytica* **214**:180.

608 **Alvarez, M. A., Li, C., Lin, H., Joe, A., Padilla, M., Woods, D. P., and Dubcovsky, J.** (2023).
609 EARLY FLOWERING 3 interactions with PHYTOCHROME B and PHOTOPERIOD1 are
610 critical for the photoperiodic regulation of wheat heading time. *PLOS Genet.*
611 **19**:e1010655.

612 **Anwer, M. U., Boikoglou, E., Herrero, E., Hallstein, M., Davis, A. M., Velikkakam James, G.,**
613 **Nagy, F., and Davis, S. J.** (2014). Natural variation reveals that intracellular distribution
614 of ELF3 protein is associated with function in the circadian clock. *eLife* **3**:e02206.

615 **Beales, J., Turner, A., Griffiths, S., Snape, J. W., and Laurie, D. A.** (2007). A Pseudo-
616 Response Regulator is misexpressed in the photoperiod insensitive Ppd-D1a mutant of
617 wheat (Triticum aestivum L.). *Theor. Appl. Genet.* **115**:721–733.

618 **Bendix, C., Marshall, C. M., and Harmon, F. G.** (2015). Circadian Clock Genes Universally
619 Control Key Agricultural Traits. *Mol. Plant* **8**:1135–1152.

620 **Benjamini, Y., and Hochberg, Y.** (1995). Controlling the False Discovery Rate: A Practical and
621 Powerful Approach to Multiple Testing. *J. R. Stat. Soc. Ser. B Methodol.* **57**:289–300.

622 **Boden, S. A., Cavanagh, C., Cullis, B. R., Ramm, K., Greenwood, J., Jean Finnegan, E.,**
623 **Trevaskis, B., and Swain, S. M.** (2015). Ppd-1 is a key regulator of inflorescence
624 architecture and paired spikelet development in wheat. *Nat. Plants* **1**:1–6.

Bucher, S. F., and Römermann, C. (2021). The timing of leaf senescence relates to flowering phenology and functional traits in 17 herbaceous species along elevational gradients. *J. Ecol.* **109**:1537–1548.

Cane, K., Eagles, H. A., Laurie, D. A., Trevaskis, B., Vallance, N., Eastwood, R. F., Gororo, N. N., Kuchel, H., and Martin, P. J. (2013). Ppd-B1 and Ppd-D1 and their effects in southern Australian wheat. *Crop Pasture Sci.* **64**:100–114.

Cao, J., Liu, H., Tan, S., and Li, Z. (2023). Transcription Factors-Regulated Leaf Senescence: Current Knowledge, Challenges and Approaches. *Int. J. Mol. Sci.* **24**:9245.

Chen, L., Hänninen, H., Rossi, S., Smith, N. G., Pau, S., Liu, Z., Feng, G., Gao, J., and Liu, J. (2020). Leaf senescence exhibits stronger climatic responses during warm than during cold autumns. *Nat. Clim. Change* **10**:777–780.

Christopher, J. T., Christopher, M. J., Borrell, A. K., Fletcher, S., and Chenu, K. (2016). Stay-green traits to improve wheat adaptation in well-watered and water-limited environments. *J. Exp. Bot.* **67**:5159–5172.

Christopher, M., Chenu, K., Jennings, R., Fletcher, S., Butler, D., Borrell, A., and Christopher, J. (2018). QTL for stay-green traits in wheat in well-watered and water-limited environments. *Field Crops Res.* **217**:32–44.

Cunningham, F., Allen, J. E., Allen, J., Alvarez-Jarreta, J., Amode, M. R., Armean, I. M., Austine-Orimoloye, O., Azov, A. G., Barnes, I., Bennett, R., et al. (2022). Ensembl 2022. *Nucleic Acids Res.* **50**:D988–D995.

Distelfeld, A., Avni, R., and Fischer, A. M. (2014). Senescence, nutrient remobilization, and yield in wheat and barley. *J. Exp. Bot.* **65**:3783–3798.

Dobin, A., Davis, C. A., Schlesinger, F., Drenkow, J., Zaleski, C., Jha, S., Batut, P., Chaisson, M., and Gingeras, T. R. (2013). STAR: ultrafast universal RNA-seq aligner. *Bioinformatics* **29**:15–21.

Dupont, F. M., Vensel, W. H., Tanaka, C. K., Hurkman, W. J., and Altenbach, S. B. (2011). Deciphering the complexities of the wheat flour proteome using quantitative two-dimensional electrophoresis, three proteases and tandem mass spectrometry. *Proteome Sci.* **9**:10.

Edelstein, A. D., Tsuchida, M. A., Amodaj, N., Pinkard, H., Vale, R. D., and Stuurman, N. (2014). Advanced methods of microscope control using μManager software. *J. Biol. Methods* **1**:e10.

Estiarte, M., and Peñuelas, J. (2015). Alteration of the phenology of leaf senescence and fall in winter deciduous species by climate change: effects on nutrient proficiency. *Glob. Change Biol.* **21**:1005–1017.

Gan, S., and Amasino, R. M. (1997). Making Sense of Senescence (Molecular Genetic Regulation and Manipulation of Leaf Senescence). *Plant Physiol.* **113**:313–319.

662 **Guo, Y., and Gan, S.** (2005). Leaf senescence: signals, execution, and regulation. *Curr. Top.*
663 *Dev. Biol.* **71**:83–112.

664 **Harmer, S. L., Hogenesch, J. B., Straume, M., Chang, H.-S., Han, B., Zhu, T., Wang, X.,**
665 **Kreps, J. A., and Kay, S. A.** (2000). Orchestrated Transcription of Key Pathways in
666 Arabidopsis by the Circadian Clock. *Science* **290**:2110–2113.

667 **Hicks, K. A., Millar, A. J., Carré, I. A., Somers, D. E., Straume, M., Meeks-Wagner, D. R.,**
668 **and Kay, S. A.** (1996). Conditional Circadian Dysfunction of the Arabidopsis early-
669 flowering 3 Mutant. *Science* **274**:790–792.

670 **Higo, K., Ugawa, Y., Iwamoto, M., and Higo, H.** (1998). PLACE: A database of plant cis -
671 acting regulatory DNA elements. *Nucleic Acids Res.* **26**:358–359.

672 **Hyles, J. E.** (2021). Genome To Phenome: Diversity For Adaptation And Phenology In Wheat
673 (Triticum aestivum L.) Advance Access published June 30, 2021.

674 **International Wheat Genome Sequencing Consortium (IWGSC)** (2014). A chromosome-
675 based draft sequence of the hexaploid bread wheat (Triticum aestivum) genome.
676 *Science* **345**:1251788.

677 **Josse, J., and Husson, F.** (2016). missMDA: A Package for Handling Missing Values in
678 Multivariate Data Analysis. *J. Stat. Softw.* **70**:1–31.

679 **Kim, H., Kim, Y., Yeom, M., Lim, J., and Nam, H. G.** (2016). Age-associated circadian period
680 changes in Arabidopsis leaves. *J. Exp. Bot.* **67**:2665–2673.

681 **Kim, H., Kim, H. J., Vu, Q. T., Jung, S., McClung, C. R., Hong, S., and Nam, H. G.** (2018).
682 Circadian control of ORE1 by PRR9 positively regulates leaf senescence in Arabidopsis.
683 *Proc. Natl. Acad. Sci.* **115**:8448–8453.

684 **Kolmos, E., Herrero, E., Bujdoso, N., Millar, A. J., Tóth, R., Gyula, P., Nagy, F., and Davis,**
685 **S. J.** (2011). A Reduced-Function Allele Reveals That EARLY FLOWERING3
686 Repressive Action on the Circadian Clock Is Modulated by Phytochrome Signals in
687 Arabidopsis. *Plant Cell* **23**:3230–3246.

688 **Lê, S., Josse, J., and Husson, F.** (2008). FactoMineR: An R Package for Multivariate Analysis.
689 *J. Stat. Softw.* **25**:1–18.

690 **Mahony, S., and Benos, P. V.** (2007). STAMP: a web tool for exploring DNA-binding motif
691 similarities. *Nucleic Acids Res.* **35**:W253–W258.

692 **Nakamichi, N., Kita, M., Ito, S., Yamashino, T., and Mizuno, T.** (2005). PSEUDO-
693 RESPONSE REGULATORS, PRR9, PRR7 and PRR5, Together Play Essential Roles
694 Close to the Circadian Clock of Arabidopsis thaliana. *Plant Cell Physiol.* **46**:686–698.

695 **Nguyen, N. T. T., Contreras-Moreira, B., Castro-Mondragon, J. A., Santana-Garcia, W.,**
696 **Ossio, R., Robles-Espinoza, C. D., Bahin, M., Collombet, S., Vincens, P., Thieffry,**
697 **D., et al.** (2018). RSAT 2018: regulatory sequence analysis tools 20th anniversary.
698 *Nucleic Acids Res.* **46**:W209–W214.

Noordally, Z. B., Ishii, K., Atkins, K. A., Wetherill, S. J., Kusakina, J., Walton, E. J., Kato, M., Azuma, M., Tanaka, K., Hanaoka, M., et al. (2013). Circadian Control of Chloroplast Transcription by a Nuclear-Encoded Timing Signal. *Science* **339**:1316–1319.

Nusinow, D. A., Helfer, A., Hamilton, E. E., King, J. J., Imaizumi, T., Schultz, T. F., Farré, E. M., and Kay, S. A. (2011). The ELF4-ELF3-LUX Complex Links the Circadian Clock to Diurnal Control of Hypocotyl Growth. *Nature* **475**:398–402.

Plautz, J. D., Straume, M., Stanewsky, R., Jamison, C. F., Brandes, C., Dowse, H. B., Hall, J. C., and Kay, S. A. (1997). Quantitative analysis of Drosophila period gene transcription in living animals. *J. Biol. Rhythms* **12**:204–217.

Ramirez-Gonzalez, R. H., Uauy, C., and Caccamo, M. (2015). PolyMarker: A fast polyploid primer design pipeline. *Bioinformatics* **31**:2038–2039.

Ramírez-González, R. H., Borrill, P., Lang, D., Harrington, S. A., Brinton, J., Venturini, L., Davey, M., Jacobs, J., van Ex, F., Pasha, A., et al. (2018). The transcriptional landscape of polyploid wheat. *Science* **361**:eaar6089.

Rees, H., Duncan, S., Gould, P., Wells, R., Greenwood, M., Brabbs, T., and Hall, A. (2019). A high-throughput delayed fluorescence method reveals underlying differences in the control of circadian rhythms in Triticum aestivum and Brassica napus. *Plant Methods* **15**:51.

Sakuraba, Y., Jeong, J., Kang, M.-Y., Kim, J., Paek, N.-C., and Choi, G. (2014). Phytochrome-interacting transcription factors PIF4 and PIF5 induce leaf senescence in Arabidopsis. *Nat. Commun.* **5**:4636.

Sanchez, S. E., and Kay, S. A. (2016). The Plant Circadian Clock: From a Simple Timekeeper to a Complex Developmental Manager. *Cold Spring Harb. Perspect. Biol.* **8**:a027748.

Simmonds, N. W. (1995). The relation between yield and protein in cereal grain. *J. Sci. Food Agric.* **67**:309–315.

Singer, J. M., and Hughey, J. J. (2019). LimoRhyde: A Flexible Approach for Differential Analysis of Rhythmic Transcriptome Data. *J. Biol. Rhythms* **34**:5–18.

Steinfort, U., Trevaskis, B., Fukai, S., Bell, K. L., and Dreccer, M. F. (2017). Vernalisation and photoperiod sensitivity in wheat: Impact on canopy development and yield components. *Field Crops Res.* **201**:108–121.

Szklarczyk, D., Kirsch, R., Koutrouli, M., Nastou, K., Mehryary, F., Hachilif, R., Gable, A. L., Fang, T., Doncheva, N. T., Pyysalo, S., et al. (2023). The STRING database in 2023: protein-protein association networks and functional enrichment analyses for any sequenced genome of interest. *Nucleic Acids Res.* **51**:D638–D646.

Thomas-Chollier, M., Herrmann, C., Defrance, M., Sand, O., Thieffry, D., and van Helden, J. (2012). RSAT peak-motifs: motif analysis in full-size ChIP-seq datasets. *Nucleic Acids Res.* **40**:e31.

Trapnell, C., Williams, B. A., Pertea, G., Mortazavi, A., Kwan, G., van Baren, M. J., Salzberg, S. L., Wold, B. J., and Pachter, L. (2010). Transcript assembly and quantification by RNA-Seq reveals unannotated transcripts and isoform switching during cell differentiation. *Nat. Biotechnol.* **28**:511–515.

Weihs, C., Ligges, U., Luebke, K., and Raabe, N. (2005). klaR Analyzing German Business Cycles. In *Data Analysis and Decision Support* (ed. Baier, D.), Decker, R.), and Schmidt-Thieme, L.), pp. 335–343. Berlin, Heidelberg: Springer.

Wittern, L., Steed, G., Taylor, L. J., Ramirez, D. C., Pingarron-Cardenas, G., Gardner, K., Greenland, A., Hannah, M. A., and Webb, A. A. R. (2023). Wheat EARLY FLOWERING 3 affects heading date without disrupting circadian oscillations. *Plant Physiol.* **191**:1383–1403.

Wu, G., Anafi, R. C., Hughes, M. E., Kornacker, K., and Hogenesch, J. B. (2016). MetaCycle: an integrated R package to evaluate periodicity in large scale data. *Bioinformatics* **32**:3351–3353.

Zhang, Y., Wang, Y., Wei, H., Li, N., Tian, W., Chong, K., and Wang, L. (2018). Circadian Evening Complex Represses Jasmonate-Induced Leaf Senescence in Arabidopsis. *Mol. Plant* **11**:326–337.

Zielinski, T., Moore, A. M., Troup, E., Halliday, K. J., and Millar, A. J. (2014). Strengths and Limitations of Period Estimation Methods for Circadian Data. *PLOS ONE* **9**:e96462.

Zikhali, M., Wingen, L. U., and Griffiths, S. (2016). Delimitation of the Earliness per se D1 (Eps-D1) flowering gene to a subtelomeric chromosomal deletion in bread wheat (Triticum aestivum). *J. Exp. Bot.* **67**:287–299.